Lyotropic Phase Behavior and Gel State Polymorphism of Phospholipids with Terminal Diene Groups: Infrared Measurements on Molecular Ordering in Lamellar and Hexagonal Phases

H. Binder,* A. Anikin,[†] G. Lantzsch, and G. Klose

Universität Leipzig, Institut für Experimentelle Physik I, Linnèstr.5, D-4103 Leipzig, Germany

Received: April 17, 1998; In Final Form: November 2, 1998

The phase behavior of the diene lipid 1,2-bis(11,13-tetradecadienoyl)-*sn*-glycero-3-phosphorylethanolamine (DTDPE) and the corresponding phosphatidylcholine analogue (DTDPC) has been studied as a function of temperature (T) and relative humidity (RH) by means of infrared (IR) dichroism measurements. Lamellar/nonlamellar and solid/fluid phase transitions of lipid films spread on an ATR crystal are determined with high resolution by means of spectral parameters. The nonlamellar inverse hexagonal (H_{II}) phase has been found for DTDPE at $T > 45$ °C, a lamellar gel at $T < 5$ °C and the lamellar liquid−crystalline phase in between at RH > 90%. The ranges of the gel and the H_{II} states can be extended into the range of moderate temperatures by dehydrating the lipid where a direct transformation between the gel and H_{II} was found. The appearance of the H_{II} phase is somewhat unexpected in view of the short effective length of the tetradecadienoyl chains. It can be attributed to the influence of the terminal diene groups which remains however unspecified. Similar to other PE lipids, DTDPE tends to transform from the gel into crystalline polymorphs. The PC analogue assembles into liquid−crystalline membranes at nearly all conditions studied. The hydration, conformation, and packing of the polar region of the lipid aggregates has been characterized by IR spectral parameters. This method has been complemented by ^{31}P NMR to assign the nonlamellar phase and by DSC to yield thermodynamic information.

1. Introduction

Diene lipids attract considerable interest because they can stabilize bilayer structures by means of polymerization.[1−3] Much effort, for instance, has been put into work devising lipid vesicles as drug delivery systems or not only to designing "artificial red cells".[4] Membranes have been modified by lipid polymerization to also yield corked,[5] ghost,[6] or skeletonized liposomes.[7,8] Depending on the location of the diene groups in the fatty acid residues, the phase behavior of the diene lipids compared to the lipid analogue without this moiety can be changed considerably as it potentially leads to perturbation.[9] Of course, the properties of the polymerized system will also depend on the location of the reactive group. Most of the related studies concentrate on lipids where the diene group is inserted into the acyl chains in a position adjacent to carbonyl moiety, i.e., near the polar/apolar interface of the lipid aggregates.[3,10−13] It has been found, for example, that the diene groups promote the formation of crystalline subgel phases by increasing the packing density within the hydrophobic core of bilayers.[12,13] Consequently, studies on diene lipids are also motivated by the question of how systems properties vary as the lipid is varied, and thus, investigations of the phase behavior of these lipids are expected to improve our basic knowledge about the stability and organization of lipid assemblies.

Beside phospholipids with choline headgroups (PC lipids) which form typically bilayer structures in an aqueous environment diene phospholipids with ethanolamine, headgroups (PE

lipids) have been synthesized to polymerize nonlamellar aggregates.[10,11] One aim of these studies would be the preparation of biocompatible interfaces. At least two aspects have to be considered in pursuing this strategy. First, the monomeric lipid should be designed to form the phases to be polymerized at moderate external conditions at which no decomposition or spontaneous polymerization of the dienic groups takes place (usually $T < 60$ °C). Second, polymerization should not destroy the lipid aggregates.

Despite the intensive and imaginative work on diene lipids leading to considerable success in preparing polymerized bilayer vesicles[3] and nonlamellar structures as inverted hexagonal (H_{II})[11] and bicontinuous cubic[10] phases, no systematic variation of the position of the diene group within the acyl chains has been performed, and with one exception,[14] only lipids with chain lengths of $n > 16$ have been synthesized. Consequently, our knowledge about the influence of the diene groups on lipids phase behavior and the properties of the respective polymers is restricted to some examples only.

The present work is devoted to the study of the phase behavior of monomeric PC and PE lipid analogues with relatively short tetradecadienoyl chains and terminal diene groups, namely, 1,2-bis(11,13-tetradecadienoyl)-*sn*-glycero-3-phosphorylcholine (DTDPC) and -ethanolamine (DTDPE). At first, we are interested in detecting the ranges of existence of nonlamellar phases which can be stimulated in general (i) by using PE lipids with a less bulky headgroup instead of PC analogues, (ii) by dehydrating the lipid, (iii) by increasing the degree of cis-unsaturation of the acyl chains, (iv) by methyl-isobranching, or (v) by lengthening of the effective chainlength.[15,16] Hence, DTDPE corresponds to the molecular property (i) but apparently contradicts (v).

[†] Lomonossow State Academy of Fine Chemical Technology, Moscow, Russia.
* To whom correspondence should be adressed. E-mail: binder@rz.uni-leipzig.de. Fax: +49-341-9732479.

CHART 1

DTDPC R = CH₃
DTDPE R = H
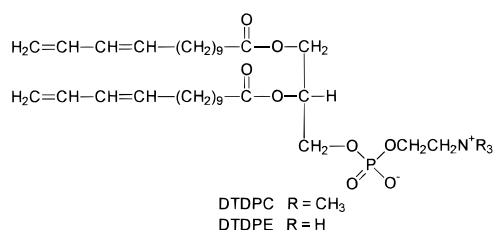
Therefore, by using the second option, we are interested to find out the specific influence of terminal diene groups on lipids phase behavior. Whereas this rigid moiety is expected to fit well into lamellar structures, its role in the formation nonlamellar aggregates is not clear. This point includes the detailed comparison of the properties of the diene lipids with that of disaturated analogues. The PC analogue DTDPC has been investigated previously to some extend.[14] Therefore we focus our study to DTDPE. The corresponding DTDPC data are supplemented only under selected aspects for comparison.

To account for reliable external conditions we chose the temperature and the relative humidity (RH) of the atmosphere surrounding the lipid. These external variables can be changed continuously, and therefore, they are well suited to induce phase transitions under well-defined conditions.[12] Vibrational spectroscopy provides macroscopic as well as microscopic information about different parts of the lipid molecules by means of semiempiric parameters. It has been proved that this method is also able to detect subtle transitions between solid and liquid−crystalline lamellar phases [12] and between lamellar and micellar phases.[17] For the determination of lamellar/nonlamellar phase transitions we applied IR linear dichroism measurements because these transformations are characterized by drastic variation of the macroscopic ordering of the molecules. ^{31}P NMR is used to identify the nonlamellar phase and DSC to get thermodynamic information.

2. Materials and Methods

Materials. 1,2-Bis(11,13-tetradecadienoyl)-*sn*-glycero-3-phosphorylcholine (DTDPC, Chart 1) was synthesized as described previously.[14] It was used as precursor for the synthesis of the corresponding PE, 1,2-bis(11,13-tetradecadienoyl)-*sn*-glycero-3-phosphorylethanolamine (DTDPE, Chart 1), by transphosphatidylation catalyzed by phospholipase D from cabbage leaves. A solution of 335 mg of DTDPC in 30 mL of ether (0.5 mM) and 200 mg of cabbage phospholipase D was added to 60 mL of 0.1 M acetate buffer containing 10% of ethanolamine and 0.1 M of CaCl₂, pH 6. The mixture was stirred overnight under argon at room temperature. After addition of 30 mL of 0.25 M solution of EDTA, lipid was extracted by a chloroform−methanol (3:1 v/v) mixture and purified by column chromatography on silica (eluant chloroform−methanol, 10:1, 3:1 v/v) yielding 205 mg (65%). The purity of the product was confirmed by TLC (chloroform−methanol−water, 65:25:4 v/v) showing a single spot on silica plates. ^{1}H NMR data of DTDPE are summarized below. The tetradecadienoyl residues of the lipids used represent originally mixtures between cis and trans isomers with a fraction of trans $f^t < 0.12$ as determined by ^{1}H NMR and IR spectroscopy.[18] Prior to the conduction of the investigations, the predominant amount of cis isomers was transformed to trans ($f^t > 0.85$) by incubating the films for 15 h at $T = 50$ °C and RH = 60%.[18] Stock solution (choloroform−methanol: 3:1 v/v; 5 mg/mL) of the lipids were used for sample preparation.

^{1}H NMR of DTDPE ((CD₃)₂SO): $\delta = 1.22$ (br, s; 24H, 2(CH₂)₆), 1,48 (m; 4H, 2(OCOCH₂C*H*₂)), 2.12 (br, quart, $J = 7.7$ Hz, 4H, 2(C*H*₂CH=)), 2.24 (t, $J = 7.2$ Hz; 2H) and 2.26 (t, $J = 7.2$ Hz; 2H) 2(OCOC*H*₂), 2.92 (m; 2H, CH₂N), 3.42 (m; 2H, CHC*H*₂OP), 3.75 (m; 2H, POC*H*₂CH₂), 4.06 (dd, $J = 12.1$ and 6.8 Hz; 1H) and 4,28 (dd, $J = 12.1$ and 3.0 Hz; 1H), (C*H*₂-OCOCH₂), 5.06 (m; 1H, C*H*OCOCH₂), 5,08 (br, d, $J = 10,5$ Hz; 2H) and 5.20 (dd, $J = 17,0$ and 2,0 Hz; 2H) 2(CH=C*H*₂), 5.42 (dt, $J = 11.0$ and 7.7 Hz; 2H, 2(CH₂C*H*=)), 5.97 (br, t, $J = 11.0$ Hz; 2H, 2(CH₂CH=C*H*)), 6.61 (dddd, $J = 17.0, 11.0, 10.5,$ and 1.0 Hz; 2H, 2(C*H*=CH₂)), 8,33 (br, s; 2H, NH₂).

TLC showed that the concentration of any impurity was less than 1 w/w %.

Infrared Dichroism Investigations. *Sample Preparation and FTIR-Measurements.* Samples were prepared by spreading 100 μL of the stock solution homogeneously on one side of a ZnSe-attenuated total reflection (ATR) crystal (50 × 5 mm, face angle 45°) and evaporating the solvent under a stream of nitrogen. The amount of lipid corresponds to a number of lipid bilayers in the order of 10^3 yielding an average thickness of the lipid film >4 μm.

The ATR crystal was mounted on a commercial horizontal Benchmark unit (Specac, Belfast, U.K.) modified in order to realize a definite RH and T at the crystal surface coated with the lipid.[12] In connection with a moisture regulating unit (HumiVar, Leipzig), this equipment allows to adjust RH continuously to values between 5% and 95% with an accuracy of about >0.5% in the temperature range (5−60)°C.

The ATR unit was placed into a BioRad FTS-60a Fourier transform infrared spectrometer (Digilab, MA) equipped with a wire grid polarizer (efficiency of >98%). Each single channel spectrum was recorded with 128 scans at two perpendicular polarizations of the IR beam which were adjusted by aligning the polarizer either parallel or perpendicular with respect to the surface normal of the ATR crystal. Polarized absorbance spectra of the sample, $A_∥(ν)$ and $A_⊥(ν)$, were calculated with a resolution of 2 cm^{-1} using the respective single channel spectra of the empty ATR crystal as background.

Although oriented lipid films form immediately when exposing the lipids to room conditions, the samples were hydrated at RH > 90% and $T = 25$ °C for at least 60 min prior to measurements. The lipids were investigated by means of increasing (hydration scan) as well as decreasing (dehydration scan) RH at constant temperature. The RH was varied in steps of 2−4%. The average scan rate used amounts to a RH change of <5%/h. In a second series of experiments the samples were investigated as a function of increasing (heating scan) and decreasing (cooling scan) temperature in steps of 1−2 K at constant relative humidity. For measurements under nearly saturated vapor atmosphere, a small vessel with distilled water was placed into the sample chamber (RH ≈ 100%). Because of imperfect sealing we cannot exclude that the real RH value is slightly smaller. The average scan rate used amounts to an effective heating/cooling rate of 1.5K/h. Before measurement the sample was allowed to equilibrate for at least 10 min after reaching the prescribed RH or T in each step. For details of equilibration see below.

Determination of the Infrared Order Parameter. The order parameter of an IR active transition moment, S_{IR}, is defined as

$$S_{IR} = \frac{1}{2}\langle 3 \cos^2 \theta_\mu - 1 \rangle \tag{1}$$

with θ_μ, which is the angle enclosed by unit vectors parallel to an individual transition moment and the normal of the crystal

Phospholipids with Terminal Diene Groups

J. Phys. Chem. B, Vol. 103, No. 3, 1999 **463**

surface. The angular bracket denotes ensemble averaging over all absorbing transition moments in the sample. If the distribution of the transition moment obeys cylindrical symmetry with respect to the normal of the ATR surface, the integral polarized absorbances of an absorption band $A_\parallel$ and $A_\perp$ are directly proportional to S_{IR},[19]

$$A_\parallel \propto K_1 + K_2 S_{IR}, \quad A_\perp \propto 1 - S_{IR} \qquad (2)$$

The constants $K_1 = 2$ and $K_2 = 2.55$ refer to an angle of incidence of 45°, a sample thickness exceeding the penetration depth of the electromagnetic waves and the ratio of the refractive indices of the sample and of the ZnSe crystal of $n_{sample}/n_{ZnSe} = 0.58$ ($n_{ZnSe} = 2.44$,[20] $n_{sample} = 1.41 \pm 0.01$[21]).[22]

Equation 2 implies that S_{IR} can be calculated from the dichroic ratio R by[19,22,23]

$$S_{IR} = \frac{R - K_1}{R + K_2} \qquad \text{with} \qquad R \equiv \frac{A_\parallel}{A_\perp} \qquad (3)$$

To exclude the effect of molecular orientations on absorption frequencies, we determined the maximum positions and the center of gravity (COG) of absorption bands from the sum spectrum $A(\nu) = A_\parallel(\nu) + K_2 A_\perp(\nu)$ that becomes independent of S_{IR} (cf. eq 2). Note, that the ATR experiment yields $A \propto (K_1 + 1) + S_{IR}(K_2 - 1)$ when using nonpolarized IR radiation. The absorbance depends on the degree of macroscopic molecular ordering in the sample in this case. The COG represents the mean frequency of an absorption bands. Due to the averaging, this parameter is sensitive to subtle variations of band position and shape with a precision (<0.2 cm^{-1}) which exceeds the spectral resolution considerably.

In case of a uniaxially symmetric molecular assembly let us introduce the unit vectors **d**, **n**, and **μ** pointing along the local director, along the normal of the ATR surface and along the respective transition moment, respectively. If the relative orientations of **d**, **n**, and **μ** are independent of each other, then S_{IR} can be written as

$$S_{IR} = S_\mathbf{d} S_\mathbf{\mu} \qquad (4)$$

where $S_\mathbf{d}$ and $S_\mathbf{\mu}$ are defined analogously as S_{IR} (cf. eq 1) but using the angles enclosed between **d** and **n** or **μ** and **d** instead of θ_μ, respectively. Consequently, $S_\mathbf{d}$ represents a measure of the degree of macroscopic ordering with respect to the ATR surface, whereas $S_\mathbf{\mu}$ quantifies the molecular ordering relative to the director of the molecular aggregate. Let us consider four special cases of molecular assemblies, namely (i) membranes aligned parallel to the ATR surface, (ii) cylinders with their axes parallel and (iii) perpendicularly to the ATR surface, and (iv) spheres. Averaging yields (i) $S_\mathbf{d}^{mem} = 1$, (ii) $S_\mathbf{d}^{cyl} = 0.25$, (iii) $S_\mathbf{d}^{cyl,\perp} = -0.5$, and (iv) $S_\mathbf{d}^{sph} = 0$, i.e., different factors which scale the local order parameter $S_\mathbf{\mu}$. Hence, a lamellar−nonlamellar phase transition is expected to cause a significant drop of the absolute value of S_{IR} because the curved shape of the lipid aggregates does not match with the plane ATR surface.

31P NMR and DSC Measurements. For NMR experiments a given amount of stock solution of the lipid was filled into glass tubes (4 mm diameter). The solvent was removed under a stream of nitrogen to yield about 8 mg of lipid. The samples were dried under vacuum and subsequently incubated for several hours at fixed T and RH which were adjusted by means of the moisture regulating unit used in the FTIR measurements. The tubes were sealed and centrifuged to deposit the lipid at the bottom of the tubes. For lipid in excess water an amount of
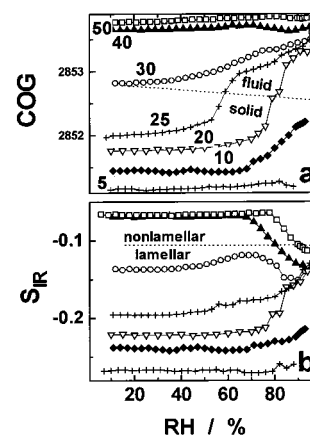

Figure 1. Center of gravity (COG, part a) and infrared order parameter (S_{IR}, part b) of the symmetric methylene stretching band ($\nu_s(CH_2)$) of DTDPE as a function of the relative humidity (RH) at different temperatures which are given in part a as numbers at the respective curves. The dotted lines separate typical parameter ranges which are attributed to different phases.

60% w/w of water was added by weighting. Spectra were recorded using a MSL-300 instrument (Bruker, Karlsruhe, Germany). The powder spectra were deconvoluted to subspectra corresponding to oriented samples with chemical shift anisotropies typical for lamellar, hexagonal, and isotropic symmetry by means of a de-Pake-ing algorithm which uses Tikhonov regularization technique.[24]

DSC measurements of the lipid (∼10 mg per sample) in excess water (50% w/w) were performed with a Perkin-Elmer DSC-7 calorimeter using heating and cooling rates of (1−2) K/min for gel/L_α transitions and 5 K/min for L_α/H_{II}. The transition enthalpies ΔH correspond to the integral of the endothermic peak over the whole transition range.

3. Experimental Results and Discussion

Solid/fluid and Lamellar/Nonlamellar Phase Transitions of DTDPE. The upper part of Figure 1 shows the center of gravity of the symmetric methylene stretching band, COG($\nu_s(CH_2)$), of DTDPE which has been progressively dehydrated at different temperatures. Typically the maximum wavenumber of the CH$_2$ stretching bands shifts upward if the conformational disorder increases.[25] A frequency increase in the range 1−3 cm^{-1} represents a diagnostic signature of the chain melting transition of lipid assemblies studied so far where the hydrocarbon chains transform from a solidlike, all-trans to a fluidlike, disordered conformation.[26] The COG($\nu_s(CH_2)$) values of DTDPE indicate that the lipid exist in a fluid state at at higher temperatures and/or humidity and in a solid state at lower T and RH. Only small hysteresis effects have been found in the hydration/dehydration experiments for the solid/fluid transitions ($\Delta RH < 4\%$).

The infrared order parameters of the symmetric CH$_2$ stretching mode $S_{IR}(\nu_s(CH_2))$ are depicted in part b of Figure 1. The negative $S_{IR}(\nu_s(CH_2))$ values indicate a preferential orientation of the acyl chain axes perpendicularly in respect to the ATR surface (see eq 1) because the transition moments of the $\nu_s(CH_2)$ vibration bisects the H−C−H bond angle of the methylene groups and consequently makes the right angle with the fiber axis of the tetradecadienoyl chains of the lipid. It is well-established that lipids in wide ranges of T and RH form bilayer membranes[27] which align spontaneously parallel to the ATR surface.[19] Comparison of both parts of Figure 1 shows that in most cases the smaller wavenumbers correlate with the
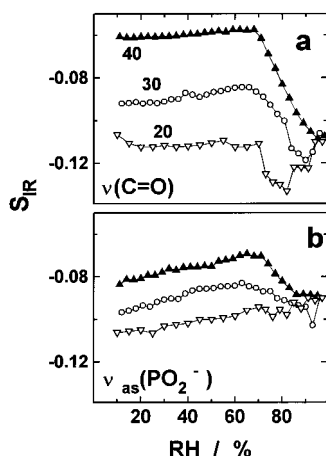
Figure 2. Infrared order parameter of the ν(C=O) (part a) and ν_{as}(PO_2^-) (part b) bands of DTDPE as a function of RH at different temperatures which are given in part a) as numbers at the respective curves.

smaller $S_{IR}(\nu_s(CH_2))$ values. We conclude that the S_{IR} values of about −0.26 to −0.23 can be attributed to a lamellar gel state. At $T = 20$ °C both, $S_{IR}(\nu_s(CH_2))$ and $COG(\nu_s(CH_2))$ increase simultaneously with progressive hydration. $S_{IR}(\nu_s(CH_2))$ levels off to values of about −0.15 indicating a considerable amount of residual ordering of the methylene chain axes. Simultaneously, the corresponding IR order parameters of the carbonyl and phosphate stretching bands, $S_{IR}(\nu(C=O))$ and $S_{IR}(\nu_{as}(PO_2^-))$, respectively, remain almost unchanged (Figure 2, see Table 1 for assignments). This finding indicates that marked modifications of the macroscopic orientation of the lipid layers can be excluded. We conclude that the lipid transforms from the gel to the liquid−crystalline phase (L_α) where the molecules with molten acyl chains remain in a lamellar arrangement. In this case the increase in $S_{IR}(\nu_s(CH_2))$ is caused predominantly by a decrease in the segmental order of the methylene units owing to the appearance of gauche defects and the enhancement of librotorsional motions about the CC bonds.

At $T \geq 40$ °C the macroscopic order of the molecules decreases distinctly upon dehydrating the lipid assembly with molten acyl chains as indicated by the parallel decrease of the IR order parameters of the methylene, the carbonyl and the phosphate groups and the essentially constant $COG(\nu_s(CH_2))$ (Figures 1 and 2). In general, membranes of phosphatidyletha-nolamines are known to transform into nonlamellar structures such as the inverted hexagonal phase (H_{II})[15,16,28−30] upon heating and/or dehydration. We suggest that the decrease of molecular orientation of DTDPE appearing with progressive dehydration and/or increasing temperature indicates the formation of a nonlamellar phase.

Supposing a transition from L_α-lamellae to H_{II}-cylinders with their axes parallel to the ATR surface. Then the absolute value of S_{IR} is expected to decrease roughly by the factor $S_d^{cyl}/S_d^{mem} = 0.25$ (see above). Hence, a residual macroscopic ordering is possible also in the nonlamellar H_{II} phase. Although relative changes in the RH-course of the IR order parameter of one sample can be detected with high precision (standard error, SE < 0.005), the values of S_{IR} varies more distinctly between independent preparations under similar external conditions (SE < 0.05) probably because of inhomogenieties of the lipid films. Therefore, the interpretation of the $S_{IR} \neq 0$ values measured in the nonlamellar range in terms of residual macroscopic ordering is questionable and requires further work.

The transition from the L_α into the nonlamellar state is accompanied by a slight increase in the position of the $\nu_s(CH_2)$

band. A similar tendency has been reported to appear at the L_α/H_{II} phase transition of DOPE.[31] It was interpreted in terms of the raised degree of disordering of the acyl chains which is caused by the increased free volume existing in the hydrophobic core of the inversely curved aggregates.

Gel State Polymorphism. The infrared spectra of DTDPE in the fluid state are reproducible unequivocally at each T and RH used. The same holds for the gel state if it has been reached by means of dehydration. Except gradual wavenumber shifts (e.g., $\nu_s(CH_2)$) and some subtle modifications of band shapes and intensities (see below) the spectra of DTDPE in the gel and fluid phases are very alike (Figure 3, spectra c and d). Under certain conditions a number of IR absorption bands of gel state samples sharpen distinctly. A similar tendency was typically found upon crystallization of lipid systems.[12,19] In these cases the maximum positions of the CH_2 stretching modes remain at relatively small wavenumbers which are typical for frozen hydrocarbon chains as noted before (see Table 1). It turns out that the spectral range 1300−700 cm^{-1} is well-suited as a fingerprint region to differentiate between the two types of crystalline DTDPE found in the experiments in addition to the gel state (see Figure 3 and Table 1): (i) The first type forms when transforming DTDPE into the gel state and storing it at a RH chosen in the intermediate range (25%-70%). We will designate this state in correspondence with previous studies[29,32] as crystalline type I, C_I (cf. spectrum a in Figure 3). (ii) The crystalline type II state C_{II} appears in some samples under similar conditions (spectrum b in Figure 3). The particular factors which are responsible for the differentiation between C_I and C_{II} are not clear. However, C_I probably refers to thermodynamic equilibrium because this form could be repro-duced easily (see below), and moreover, C_{II} polymorphs after cycling over the melting transition transform into C_I in most cases.

The marked variations of the C_I and C_{II} state spectra in comparison with the gel are related most of all to vibrations of the polar groups of the lipid (see Figure 3 and Table 1 for assignments). Interestingly, bands originating from the phosphate and ammonium groups are affected more drastically in the C_I state {notice, for example, the sharpening of $\nu_s(PO_2^-)$, $\nu_s(P-(OC)_2)$, $\delta_s(NH_3)$, $\nu_s(CCN^+)$, and $\delta(CCN^+)+\delta_s(NH_3)$)}, whereas IR absorption of the ester group show a characteristic pattern in the C_{II} state (e.g., sharpening of $\nu_{as}(COC)$, $\nu_s(COC)$, and splitting of $\nu(C=O)$). Note that C_{II} type spectra retain some features of the C_I state and thus possibly represent a superposi-tion of two crystalline species similar to the L_c phase intermedi-ates of diacyl PEs reported by Lewis and McElhaney.[29]

A considerable degree of correspondence can be established between the solid states of DTDPE and the three types of spectroscopically distinct polymorphs found in disaturated PEs with acyl chains containing $n < 17$ carbons.[29,32] They form an isostructural series which shows no evidence for any chain-length-dependent differences in the structure and organization of the polar/apolar interface. The presence of the diene moieties obviously does not (or only weakly) affect the crystallization properties of the ethanolamine headgroups. They are known to form a very rigid network which does not require water molecules owing to direct H bonds between the ammonium and phosphate groups.[33,34]

The crystallization of DTDPE is accompanied by the gradual decrease in the integral intensity of the broad O−H stretching band of the water adsorbed onto the lipid indicating a consider-able dehydration of DTDPE upon crystallization. For example, this broad feature spanning the range 3700−2400 cm^{-1} weakens

Phospholipids with Terminal Diene Groups

J. Phys. Chem. B, Vol. 103, No. 3, 1999 **465**

TABLE 1: Assignments of Selected Absorption Bands of DTDPE and the Corresponding Wavenumbers at Maximum Absorbance in the Fluid (L$_\alpha$, H$_{II}$) and Solid (gel, C$_I$ and C$_{II}$) States[b]

group vibrations	assignment	symbol	wavenumber/cm^{-1}			
			L$_\alpha$/H$_{II}$	gel	C$_I$[d]	C$_{II}$[d]
methylene	antisymmetric stretching	$\nu_{as}(CH_2)$	2924	2920	2918	2917
	symmetric stretching[c]	$\nu_s(CH_2)$	2854 (−0.18)	2851 (−0.25)	2851 (−0.20)	2849 (>−0.14)
	bending	$\delta(CH_2)$	1465	1466	1464, 1472 sh	1470 sp
	rocking	$\gamma_r(CH_2)$	722	722	721, 727 sh	719
carbonyl	C=O stretching	$\nu(C=O)$	1739	1740	1742	**1733** vs, 1741 sh
						1718 sh
	C−O−C antisymmetric stretching	$\nu_{as}(COC)$	1174 br	1179 br	1177	**1180** sp
	C−O−C symmetric stretching	$\nu_a(COC)$	ol	ol	ol	**1063**
phosphate	PO$_2^-$ antisymmetric stretching	$\nu_{as}(PO_2^-)$	1222[a]	1227[a]	1224 sp	1222 sp
	PO$_2^-$ symmetric stretching	$\nu_s(PO_2^-)$	1073	1075	**1081** sp	1084
	P−(OC)$_2$ antisymmetric stretching	$\nu_{as}(P−(OC)_2)$	824 br	825 br, 803 sh	822, 802	815, 805
	P−(OC)$_2$ symmetric stretching	$\nu_s(P−(OC)_2)$	759 br	760 br, 743 sh	**760** sp, **740** w	759, 740
ammonium	combination of CCN$^+$ bending and $\delta_s(NH_3)$	$\delta(CCN^+)+\delta_s(NH_3)$	/2090 br	2125 br	**2135** sp	2120
	N$^+$H$_3$ antisymmetric bending	$\delta_{as}(NH_3)$	1638	1636	1633	1632
	N$^+$H$_3$ symmetric bending	$\delta_s(NH_3)$	1530 br	1540 br	**1561** sp	1579, 1563 m
	CCN$^+$ antisymmetric stretching	$\nu_{as}(CCN^+)$	1026 br	1029 br	1014 w	1016 s, 983 m
	CCN$^+$ symmetric stretching	$\nu_s(CCN^+)$	ol	ol	**917** s	ol

[a] Maximum shifts with progressive dehydration. [b] Abbreviations: br, broad; sp, sharp; s, strong; vs, very strong; m, medium; w, weak; sh, shoulder; ol, overlapped by neighboring bands. Assignments of group vibrations are taken from references.[19,29] Peaks are resolved to whole wavenumbers. [c] The corresponding IR order parameter is given in parentheses. [d] The boldface numbers emphasize bands which are characteristic for the respective crystalline form.
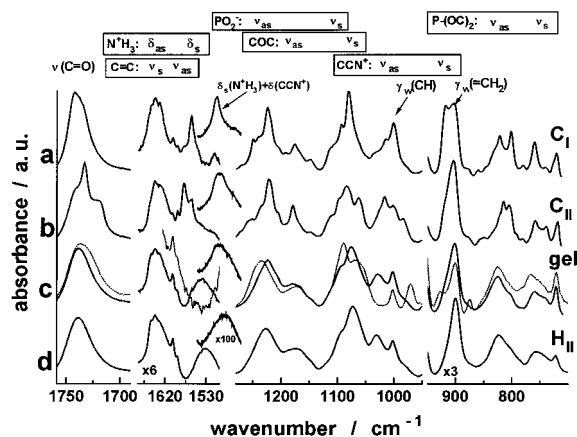

Figure 3. Selected regions of the infrared absorbance spectra of DTDPE corresponding to different solid polymorphs (parts a−c, designations are given at the right) and to the nonlamellar H$_{II}$ phase (part d). In part c, the gel state spectrum of the PC analogue DTDPC is drawn for comparison (dotted). Selected absorption bands are assigned at the top of the figure (see also Table 1). The spectral range 2260−1980 cm^{-1} with the combination band $\delta_s(N^+H_3)+\delta(CCN^+)$ is drawn without abscissa as insert close to the $\nu_s(N^+H_3)$ band for comparison. The experimental conditions are RH = 50%, T = 15 °C for the C$_I$, C$_{II}$, and gel states of DTDPE (see text for equilibration conditions), RH = 50% and T = 50 °C for the H$_{II}$ phase and RH = 10% and T = 10 °C for the gel state of DTDPC.

by about 25% when transforming DTDPE from the gel into the C$_I$ state at RH = 50%. We conclude that the sharpening of phosphate and ammonium bands in the C$_I$ state can be attributed to an immobilization of the PE moieties which is caused by the partial replacement of water−PE contacts by well-localized, direct interactions between the headgroups of adjacent lipid molecules. Lewis and McElhaney [29] suggest that the amine protons are "locked" in long-lived hydrogen bonds with phosphate groups giving rise to sharp NH$_3^+$ bending bands. This effect is accompanied by relatively small frequencies of the PO$_2^-$ stretching modes (when compared with the PC, see below) indicating H bonding.

The dehydration of the lipid in the C$_{II}$ state is of the same order of magnitude as that in the C$_I$ state; however, in this case

the spectral changes of the C=O and COC stretching modes suggest marked modifications of hydration and/or conformation of the lipid in the region of the carbonyl groups. The carbonyl stretching band of the C$_{II}$ form is clearly the composite of at least three bands (Figure 3 and Table 1). The bands at 1741 and 1733 cm^{-1} probably arise from populations of free and hydrated (i.e., hydrogen-bonded) ester carbonyl groups, respectively.[35] The additional low-frequency band (1718 cm^{-1} in DTDPE) has been assigned hypothetically to C=O groups in the *sn*-2 chains which are hydrogen-bonded to amine protons of the PE headgroup.[29] Thus, in contrast to the C$_I$ form, the carbonyl groups in the C$_{II}$ crystals are obviously exposed to pronounced H bond formation.

Crystalline type I spectra of disaturated PEs exhibit crystal field splitting of the methylene bending and rocking bands which is characteristic for acyl chains packed in an orthorhombic subcell.[29,32] A marked splitting of these bands is not obvious in the spectra of the C$_I$ form of DTDPE. However, a distinct broadening of the $\delta(CH_2)$ mode, a downward shift of its maximum and the appearance of a shoulder at the left flank, can be interpreted as an indication of a weak crystal field splitting (cf. Table 1, note the analogous tendency of the methylene rocking mode). Thus, the tetradecadienoyl chains of DTDPE obviously tend to arrange into an orthorhombic perpendicular crystalline subcell, the degree of ordering of which is, however, less perfect than that formed by acyl chains of disaturated PEs. Analogous to the crystalline type II spectra of disaturated PEs,[29,31] the methylene bending band of the C$_{II}$ form of DTDPE represents a narrow singlet which is located however at a relatively high wavenumber of 1470 cm^{-1}. Mantsch et al. attributed this finding to a more loosely packed hexagonal subcell.[31] We note, however, that a slight upward shift and narrowing of the $\delta(CH_2)$ mode is characteristic for the parallel alignment of the polymethylene planes in a densely packed triclinic subcell as observed, e.g., in the subgel phase of DPPC.[36] We prefer this interpretation because a dense packing of the polymethylene chains would correspond to the spectral properties of the C=O and COC (see below) stretching modes which indicate a high degree of ordering of these moieties. Interestingly, the positions of absorption bands originating from the
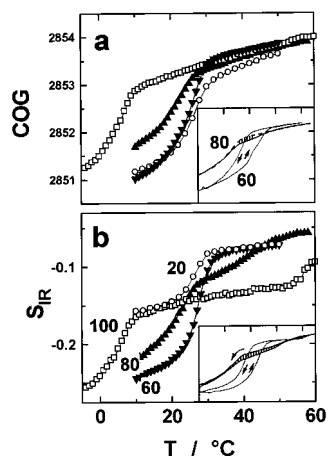
Figure 4. Center of gravity (COG, part a) and infrared order parameter (S_{IR}, part b) of the symmetric methylene stretching band ($\nu_s(CH_2)$) of DTDPE as a function of the temperature (T, cooling scans) at different RHs which are given in part b as numbers at the respective curves. Heating and cooling scans at RH = 60% and 80% are given in the insertions to indicate hysteresis effects. RH = 100% corresponds to saturated vapor atmosphere.
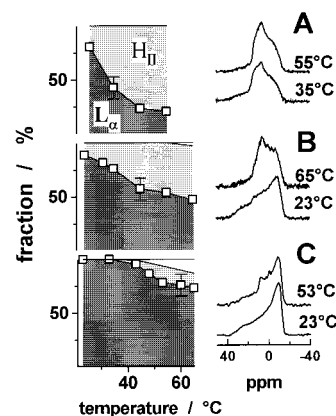

Figure 5. Representative ^{31}P NMR spectra of (spectrum A) DTDPE hydrated at $T = 50$ °C/RH = 50%, (spectrum B) 25 °C/92%, (spectrum C) and of DTDPE in excess water (60% w/w water). The fractions of the lipid existing in the L_α (gray), H_{II} (light gray) and isotropic (white) state are shown as a function of the temperature in the left part of the figure. The data represent the fractional areas of peaks of the de-paked ^{31}P NMR spectra having a mean chemical shift anisotropy of $\sim -30 \pm 5$ ppm (L_α), $\sim +15 \pm 3$ ppm (H_{II}) and $\sim 0 \pm 3$ ppm (isotropic) (not shown).

diene groups are not affected significantly by the phase state of the lipid (Figure 3).

The infrared order parameters of the methylene stretching bands indicate that the degree of macroscopic ordering is reduced in the C_{II} state ($S_{IR}(\nu_s(CH_2)) > -0.15$). Possibly this effect is caused by the rearrangement of the lipid into a nonlamellar structures as, for example, the inverted form of the so-called ribbon phase P_δ, which is thought to be constructed by strains of headgroup-centered lipid assemblies having a ellipse as the cross section.[28] This phase has been reported for almost dry DPPE, DPPC, and DOPE.[37,38]

Equilibration and Hysteresis Effects: Temperature Scans. Cooling scans of the FTIR samples are performed at constant RH. The temperature behavior of the spectral parameters COG-($\nu_s(CH_2)$) and $S_{IR}(\nu_s(CH_2))$ (Figure 4, parts a and b, respectively) yields a consistent picture when compared with the results of the dehydration scans presented above.

Heating and cooling scans which are recorded at RH > 70% show small hysteresis effects at the solid/fluid transition (Figure 4, insets). At RH ≤ 60%, the melting of the acyl chains at the gel/nonlamellar transition shifts however markedly by about 5 ± 1 K upward in contrast to freezing when comparing the inflection points of the COG($\nu_s(CH_2)$) curves (Figure 4, insertions). This hysteresis was found to remain unchanged even at scan rates which are 2 times slower. Detailed inspection of the IR spectra reveals that upon heating the lipid starts to transform slowly from the gel into the C_I polymorph before melting. We suggest that the delayed melting is caused by the stronger intermolecular interactions in the crystalline lipid.[15,29,32] Moreover we conclude that the gel state of DTDPE reached in the dehydration and cooling scans is metastable, whereas the crystalline C_I state corresponds to thermodynamic equilibrium. The gel/C_I transition is inhibited or slowed if one stores the lipid at RH < 25%. This finding is in close agreement with the gel−subgel equilibration kinetics of a dienic PC studied recently at different RH.[12] In general we found that the relaxation times of the lipid are in the order of days (or longer) for solid, dry samples (RH < 25%), on the order of hours for solid samples in the intermediate RH range and in the order of minutes (or shorter) for fluid samples. Thus, it appears convenient to examine the gel/L_α phase transition in the cooling or dehydration

mode since they enable a better control over the rate of lipid crystallization.

Identification of the Nonlamellar Phase: ^{31}P NMR Measurements. ^{31}P NMR spectra of samples were recorded at different temperatures to identify the nonlamellar phase of DTDPE. Prior to measurements the samples were hydrated at a definite RH and T and sealed: Sample A was equilibrated at conditions where the nonlamellar phase was detected by IR, sample B at conditions where lipid lamellae dominate, and sample C in excess water. Typical data sets displaying the temperature-dependent changes are illustrated in Figure 5. At room temperature the samples B and C exhibit the axially asymmetric powder pattern of a lamellar lipid assembly.[39,40] Upon further heating a second feature of reduced width and reversed asymmetry appears. This type of powder pattern is typical for H_{II} phases in phospholipid assemblies.[41,42] In addition, a narrow isotropic resonance is detected in sample C at $T > 50$ °C, an indication of complex structures with high curvature, e.g., small particles of lamellar or cubic phases. The ^{31}P NMR spectra of the sample with the smallest water content (A) indicate a dominating H_{II} component at $T > 30$ °C. The spectra are reproducible after reversed cooling of the samples.

To determine quantitatively the fractional intensities of the overlapping signals the powder spectra were de-Pake-ed. The fraction of lipid in H_{II} structures increases with increasing T and decreasing water content (Figure 5). This tendency agrees with the results of the infrared dichroism measurements which reveal the existence of the nonlamellar phase at similar conditions.

Although the origin of the isotropic peak cannot be assigned by the results of our investigations, we note that cubic phases exist in a number of amphiphilic systems in the range of external conditions between that of the lamellar and inverted hexagonal phases.[28] The free energy per lipid molecule is very similar in cubic and H_{II} structures giving rise to metastability problems where either both or one of the phases form in dependence on the handling of the sample.[10,43−45] Note that the FTIR parameters are highly reproducible in the nonlamellar phase range. That means we have no indications of phase coexistence and metastability in the FTIR samples which represent a thin film of an average thickness of only several micrometers. In contrast,

Phospholipids with Terminal Diene Groups

J. Phys. Chem. B, Vol. 103, No. 3, 1999 **467**

TABLE 2: Calorimetric Phase Transition Temperatures and Enthalpies and Entropies of DTDPE and DTDPC in Excess Water

lipid	transition	$n_0{}^a$	$T_{m,h}$ °C		$\Delta H_{m,h}$ kJ/mol		$\Delta S_{m,h}$ J/(mol K)	
			DSC^e	predicted	DSC^e	predicted	DSC^e	predicted
DTDPE	gel/L$_\alpha$	8−9	4.5	4^b	14	11^b	52	39^b
	L$_\alpha$/H$_{II}$	12−13	45	95^c	0.7	1^b	2	2^b
DTDPC	gel/L$_\alpha$		−21/−16	−25^d	13	13^d	51	53^d

^{a} Numbers of methylene segments in disaturated PEs at which the transition enthalpy and entropy extrapolate to zero.[16] ^{b} According to the empirical relations derived for disaturated PEs, $T_m \approx 385K(1 - 0.9/(n - 7.8))$; $\Delta H_m \approx 2(2.34(n - 20.35))$kJ/mol; $\Delta S_m \approx 2(6.07(n - 47.3))$J/(mol K); $\Delta H_h \approx 2(0.25(n - 3.05))$kJ/mol and $\Delta S_h \approx 2(0.71(n - 8.9))$J/(mol K); assuming a length of $n = 11$ carbons per chain for the main phase transition and $n = 14$ for the lamellar/hexagonal phase transformation.[16] ^{c} According to a linear relation derived from the data given in ref 15; $T_h \approx T_m + ((290 - 14.3n_{eff}))$ K assuming an effective chainlength $n_{eff} = 14$. ^{d} Assuming a difference between PC and PE data as for di-C$_{12}$ lipids.[37] ^{e} SE: T_{PT}, ±1K, ΔH ±1kJ/mol; ΔS, ±5J/mol K. FWHM of the peaks: gel/L$_\alpha$, 4 K, L$_\alpha$/H$_{II}$, 10 K; the data represent mean values of heating and cooling scans.

the NMR samples are much more bulky and probably are more difficult to equilibrate. The determination of respective equilibrium phase diagrams is complicated by the presence of slow kinetics which broaden the phase coexistence region.[43] The systematic characterization of the stability and interconversion of nonlamellar phases in theses bulky samples is not the focus of this paper. The essential result of the NMR experiments is the detection of a predominant fraction of H$_{II}$ aggregates at external conditions where the FTIR measurements give evidence of a nonlamellar phase. The phase ranges are precisely determined by infrared spectroscopy and, in particular, by linear dichroism measurements.

X-ray diffraction measurements of DTDPE films on glass slides indicate a series of equally spaced Bragg peaks at external conditions which has been attributed to the L$_\alpha$ and gel states by means of the FTIR experiments. In the nonlamellar range a characteristic change of the diffraction pattern has been observed giving further evidence of the H$_{II}$ phase. The results of X-ray experiments will be published separately to characterize the dimensions of the DTDPE aggregates.

Phase Transitions in Excess Water: DSC Measurements. DSC heating scans of DTDPE in excess water indicate an intense endothermal event centered at ∼5 °C. It can be assigned to the gel/L$_\alpha$ transition found at the same temperature in the infrared measurements (Figure 4, RH = 100%). The transition temperature, enthalpy and entropy of the main transition (T_m, ΔH_m, and ΔS_m, respectively) agree fairly well with values which are predicted from the respective chainlength dependence of a homologous series of disaturated PEs,[16] see Table 2. The assumption of $n = 11$ carbons per chain takes into account the nine CH$_2$ groups per tetradecadienoyl chain in DTDPE. Obviously the terminal diene groups have only a small effect on the melting of the polymethylene part of the acyl chains.

The gel/L$_\alpha$ transition data of DTDPC confirm this conclusion (Table 2). The corresponding endothermic event represents however the composite of two subpeaks centered at ∼−21 °C and at ∼−16 °C. The origin of this phenomenon is not clear and is now under study. Note that DTDPC exhibits the gel/L$_\alpha$ transition below the freezing point of water where the lipid lamellae exist in equilibrium with ice. It is known that the gel/L$_\alpha$ phase transition of lipids in the presence of ice can cause a certain number of water molecules to melt and to associate with the lipid headgroups as soon as the lipid has passed through the chain melting transition.[46,47] Possibly this effect contributes to the endothermograms of DTDPC.

DSC scans of DTDPE recorded with an increased rate of 5K/min reveal a second, much weaker and broader endothermic event centered at 45 °C which can be assigned, probably, to the liquid−crystalline/inverted hexagonal phase transition. The enthalpy and entropy of this transition, ΔH_h and ΔS_h, agree with the predictions which can be made on the basis of L$_\alpha$/H$_{II}$

transition data of disaturated PEs if one assumes $n = 14$ (Table 2). This finding confirms the idea of Lewis et al. who showed that the effective chain length of PE lipids plays an important role for the L$_\alpha$/H$_{II}$ phase transition.[15] The effective chain length n_{eff} is defined by the total number of carbons in the "main chain" which is indeed $n_{eff} = 14$ for DTDPE. PEs of a given n_{eff} exhibit their L$_\alpha$/H$_{II}$ transition at a relatively constant temperature interval above T_m. From the data given in reference[15] one can extrapolate an expected difference of the transition temperatures, $T_h - T_m$, (T_h is the L$_\alpha$/H$_{II}$ transition temperature) for $n_{eff} = 14$ which overestimates however the observed value distinctly (Table 2). Moreover, L$_\alpha$/H$_{II}$ transitions are not detected typically for $n_{eff} < 15$.[15,16] The terminal diene groups obviously stabilize the lipid aggregates and thus, promote the formation of inverse hexagonal structures. One can suggest that these moieties restrict the flexibility of the terminal part of the acyl chains. In general, the formation of the H$_{II}$ phase appears to be driven by a delicate balance between the spontaneous curvature of the lipid monolayers, the interactions between opposite bilayers in multilamellar stacks and the energy costs of the formation of interstices.[48] A molecular interpretation of the role which the terminal diene groups play is still open and will be studied separately.

The FTIR measurements on DTDPE at RH = 100% yield the L$_\alpha$/H$_{II}$ transition at a temperature increased by more than 10 K when compared with that suggested from the DSC scans (Figure 4, part b). For DSC measurements we used bulk probes as for NMR and therefore this difference is caused possibly by any unspecified influence of the solid support in the IR preparation (see discussion in the previous paragraph). On the other hand, one can suggest that the relative humidity in the sample chamber even in the presence of a water reservoir is slightly below 100% because of a not perfect sealing. FTIR heating scans of DTDPE in excess water reveal a loss of macroscopic ordering of the lipid at $T = 45-55$ °C in agreement with the DSC results. Note, however, that the thorough study of DTDPE at temperatures $T > 50$ °C in excess water is complicated by the onset of polymerization and/or decomposition of the diene groups as reported previously.[14] In view of these difficulties it appears reliable to assign the L$_\alpha$/H$_{II}$ transition of DTDPE at full and nearly full hydration to temperatures in the range 45−60 °C. Note that the conclusion about the stabilizing effect of the diene groups on H$_{II}$ formation is not affected by this uncertainty.

Phase Diagram of DTDPE. On the basis of the phase assignments which are obtained by means of the ^{31}P NMR measurements on one hand and the phase transition data of the FTIR and DSC experiments on the other, we are able to construct the T−RH phase diagram of DTDPE (Figure 6). We assign the nonlamellar phase to H$_{II}$ provided that the appearance of small amounts of other nonlamellar structures as, for example,
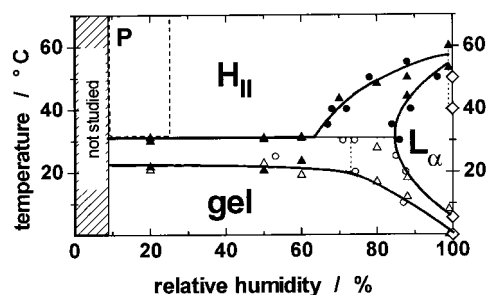
Figure 6. T−RH phase diagram of DTDPE.. The onset and completion temperature/humidity (triangles/circles, respectively) of the phase transitions are determined from the intersection points of lines which are fitted to the pure-phase and coexistence ranges of the cooling/dehydration scans of COG (open symbols) and S_{IR} (solid symbols) of the $\nu_s(CH_2)$ band. The respective data for excess water conditions (drawn at RH = 100%) are taken from the DSC scans (diamonds). The borderline between the (gel+H_{II}) and (gel+L_α) is hypothetical (vertical dotted line). Preliminary X-ray studies suggest lipid tubules with a distorted cross section in the range that is denoted by P. The exact L_α/H_{II} transition temperature in excess water and at RH $\approx$ 100% are not clear yet (dotted line).

Figure 7. (part a) Center of gravity (COG) of the $\nu(C=O)$, (part b) $\nu_{as}(PO_2^-)$ and (part c) $\nu_{as}(COC)$ bands of DTDPC (solid symbols, $T = 25$ °C) and of DTDPE (open symbols, temperatures are indicated in part c) as a function of RH. The left axis refers to the PE and the right to the PC.

cubic phases, cannot be excluded. Furthermore, X-ray data show that the hexagonal cylinders seem to distort into ribbons in a rectangular arrangement at low RHs (RH < 30%). This effect will be discussed in a separate publication.

The sigmoidal courses of center of gravity COG($\nu_s(CH_2)$), and IR order parameter $S_{IR}(\nu_s(CH_2))$ yield the characteristic transition points of the solid−fluid and lamellar−nonlamellar transitions, respectively (cf. legend of Figure 6). The phase diagram shown in Figure 6 was obtained from the dehydration and cooling scans. Its liquidus and solidus lines refer to the onset and completion of the phase transition. The heating scans yield solidus and liquidus lines that are shifted by ~5K toward higher temperatures at RH < 70% owing to the hysteresis effects (not shown).

The parallel changes of COG($\nu_s(CH_2)$) and $S_{IR}(\nu_s(CH_2))$ give evidence of the direct conversion between the solid−lamellar and the fluid−nonlamellar state at RH < 70% (cf. Figure 1, phase sequence gel → H_{II}). The formation of fluid lamellae (L_α phase) at intermediate temperatures (phase sequence gel→L_α→H_{II}) can be ruled out owing to the drastic decrease of the macroscopic acyl chain ordering. Gel/H_{II} transitions are reported for disaturated long chain PEs in excess water (22:0, refs 45 and 49) and in saturated salt solution (18:0 and 20:0, ref 16) and for several PEs at limited hydration.[16,28,37,45]

The phase behavior of the PC analogue of DTDPE has been examined by means of DSC in excess water (see above) and infrared spectroscopy in the range of external conditions 50 °C > T > −10 °C and 98 > RH > 5% (data not shown). These measurements reveal that DTDPC exists predominantly in the L_α phase at T > 0 °C and RH > 50%.

Water/Lipid Interactions: Carbonyl and Phosphate Group Vibrations. The centers of gravity of the phosphate, and carbonyl stretching bands of DTDPE, COG($\nu_{as}(PO_2^-)$), and COG($\nu(C=O)$), respectively, shift monotonically toward lower wavenumbers upon increasing hydration at all temperatures studied (Figure 7, parts a and b). This behavior has been found in a large number of lipid systems, and it was attributed mainly to the progressive hydrogen bonding of water to the phosphate and carbonyl moieties.[19,23,35,50-55] Typically, the COG courses measured at $T \geq 40$ °C can be divided into two nearly linear parts with a break at the onset of the H_{II}/L_α phase transition. The smaller slope of the initial part can be interpreted as an indication of the decreased hydration of the lipid in the H_{II} phase
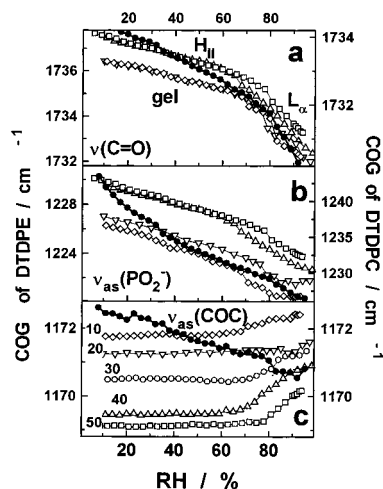
range. Obviously this tendency affects the carbonyl groups and the phosphate groups as well. The weakening of hydrogen bonding to these groups upon temperature induced H_{II} formation has been concluded from the upward shifts of the $\nu(C=O)$) and $\nu_{as}(PO_2^-)$ bands of PE lipids.[56] Analogous changes of the $\nu(C=O)$) frequency without shifting of the $\nu_{as}(PO_2^-)$ band has been reported earlier in PE/water suspensions.[31,57] Comparison of the COG curves at constant RH gives rise to the conclusion that the temperature has only a little effect on the COG data in the one-phase ranges whereas the COGs differ distinctly if the data correspond to different phases of the lipid.

Note, that the positions of the ammonium bending vibration $\delta_s(N^+H_3)$ and of the combination band $\delta_s(N^+H_3)+ \delta(CCN^+)$ differ significantly in the fluid lamellar and hexagonal phases (cf. Table 1 and Figure 3). The shift toward smaller wavenumbers indicates that also the N^+H_3 groups are affected upon L_α/H_{II} transformation by sterical restrictions and/or modifications of water−ammonium interactions.

The RH courses of the respective COGs of the PC analogue with tetradecadienoyl chains DTDPC are also drawn in Figure 7 for comparison using solid symbols (please note the right ordinate axis which is extended in part b and shifted in part a). In our representation the absolute values of the COG as well as the slope of their almost linear courses can be interpreted as a measure of water−polar group interaction. The steeper negative slopes of the COG($\nu_{as}(PO_2^-)$) and COG($\nu(C=O)$) curves of DTDPC reflect the fact that the PC headgroups are highly hygroscopic, whereas the PE groups are more difficult to hydrate. The absolute values of the COG($\nu(C=O)$) of DTDPC are about 3 cm^{-1} smaller than that of DTDPE the carbonyl groups of which are obviously more strongly screened from the water in comparison with the PC (compare also the spectra of DTDPE and DTDPC in Figure 3, part c). On the other hand, the $\nu_{as}(PO_2^-)$ band of the PE appears at distinctly smaller wavenumbers suggesting stronger hydration in contradiction with the other findings. Alternatively, it appears more probably that direct ammonium-phosphate interactions between the PE headgroups are responsible for the downward shift of the $\nu_{as}(PO_2^-)$ frequency in a similar fashion as suggested above for the crystalline polymorphs. Note that also the symmetric stretching mode $\nu_s(PO_2^-)$ of DTDPE is shifted toward smaller wavenumbers in comparison with the PC (cf. Figure 3, part c).
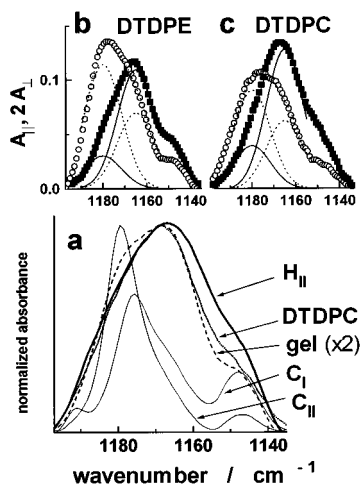
Figure 8. Infrared absorbance spectra of the dienic lipids in the region of the ν_{as}(COC) band after base line correction. Characteristic sum spectra of the different phases of DTDPE and of DTDPC in the solid state (the respective conditions are given in the legend of Figure 3) are drawn in part a. Polarized absorbance spectra $A_{\|}(\nu)$ (open circles) and $2A_{\perp}(\nu)$ (solid squares) of the lipids in the gel state are shown in part b (DTDPE) and part c (DTDPC). Each polarized ν_{as}(COC) band has been fitted by a superposition of two Gaussian functions of free adjustable intensity centered at 1180 cm^{-1} and at 1165 cm^{-1}, respectively (common bandwidth 20 cm^{-1}). The functions fitted to $A_{\|}(\nu)$ and $2A_{\perp}(\nu)$ are drawn by dotted and solid lines, respectively. Note that the shoulder at about 1147 cm^{-1} originates from the antisymmetric stretching of the C−O−P ester bond.

Lipid Conformation at the Polar/Apolar Interface: Carbonyl- Ester Bond Vibrations. The COG of the antisymmetric ester bond stretching band ν_{as}(COC) of DTDPC decreases linearly with increasing RH as expected because a stretching mode usually shifts toward lower frequency with increasing polarity in the surroundings of the vibrational entity (Figure 7, part c). Consequently, the nearly constant values of the COG(ν_{as}(COC)) curves of the PE analogue which even start to increase at the onset of H$_{II}$/L$_{\alpha}$ coexistence are somewhat unexpected. A similar upward shift of the ν_{as}(COC) frequency has been observed upon formation of cubic phases in the system monooleylglycerol−water with increasing water content.[51,58] We suggest in accordance with the interpretation given by the authors for their system that the high sensitivity of the ν_{as}(COC) mode for the nonlamellar/lamellar transformation of DTDPE is caused by changes of the conformation and/or packing in the vicinity of the ester groups. This moiety is located at the polar/apolar interface of the aggregates, i.e., just at a position which is expected to be exceptionally sensitive for mesomorphic changes.

The inspection of the polarized spectra in the region of the ν_{as}(COC)) feature reveals the existence of two differently polarized subbands (Figure 8, parts b and c). The left-hand and right-hand component bands of DTDPE in the gel state yield order parameters of $S_{IR}(\nu_{as}^1$(COC)) = +0.55 ($\langle\theta\rangle$ = 33°) and $S_{IR}(\nu_{as}^2$(COC))= −0.19 (63°), respectively (see the caption of Figure 8 for details of data analysis). The values in the parentheses are the corresponding mean inclination angles of the transition moment with respect to the membrane normal (cf. eq 1). The transition moment of the ν_{as}(COC) mode can be assumed to point from C$_2$ to the ester oxygen in the C$_2$−(C$_1$=O)−O fragment.[59] Hence, the infrared order parameter $S_{IR}(\nu_{as}$(COC)) gives a measure of the orientation of the acyl chain axis at the position of the ester link to the glycerol moiety. Usually the two ester groups of (1,2)-diacetylene lipids adopt nonequivalent orientations in membranes where the axis of the

ester group in the *sn*-2 position inclines from the membrane normal and that in the *sn*-1 position is directed along the bilayer normal.[27] In view of this property the obtained data appear plausible if one assigns the low-frequency subband 2 to the ester group in the *sn*-2 position and the high-frequency band 1 to that in the *sn*-1 position. Infrared dichroism measurements on selectively ^{13}C=O(*sn*-2) labeled DMPC and DPPC have given evidence that the two CO−O ester bonds are oriented very differently.[23] The reported $S_{IR}(\nu_{as}$(COC)) and $S_{IR}(\nu_{as}(^{13}$COC)) values for the gel state of 0.59 (*sn*-1) and −0.15 (*sn*-2) are in very good agreement with the IR order parameters of DTDPE obtained by means of band separation.

Infrared experiments on crystalline tripalmitin showed that the ν_{as}(COC) band is centered around 1180 cm^{-1} when the C$_3$−C$_2$−C$_1$O−O−C segments of the ester chains adopt a planar all-trans conformation.[60] Deviations from this conformation in the molten state shift this band down to ∼1170 cm^{-1}. Consequently the frequency shift between the ν_{as}(COC)) component bands of DTDPE can be explained by the different conformation of the C$_3$−C$_2$−C$_1$O−O−C fragment which is nearly all-trans in the *sn*-1 position (ν_{as}^1(COC) at 1180 cm^{-1}) but distinctly distorted in the *sn*-2 position in order to realize a downward bend of the acyl chain axis (ν_{as}^2(COC) at 1165 cm^{-1}). X-ray crystal analyses of membrane lipids yield dihedral angles in the range −80° to −135° for rotations about the C$_2$−C$_1$ bond in the *sn*-2 chain.[61] The order parameters of the component bands of DTDPC in the gel state ($S_{IR}(\nu_{as}^1$(COC)) = +0.34 $\langle\theta\rangle$ = 42°) and $S_{IR}(\nu_{as}^2$(COC)) = −0.28 (67°)) give evidence of a similar orientations of the CO−O−C fragments in the PC and PE bilayers.

The two component nature of the ν_{as}(COC) band suggests that the COG changes reported above (Figure 8, part c) result mainly from variations of the fractional intensities of the component bands and to a less extend from a shift of their maximum positions (see also ref 62). Indeed, the positions of the subbands are found to remain nearly fixed at ∼1165 and ∼1180 cm^{-1} in membranes of DTDPE and DTDPC at different degrees of hydration. That is, the downward shift of the COG(ν_{as}(COC)) of DTDPC can be attributed to an increasing fractional absorbance of the right-hand component with increasing RH. Although a quantitative analysis of the fractional intensities of the subbands is not appropriate due to their unknown extinction coefficients, one can conclude on a qualitative basis that this effect is caused by an increase in the fraction of disordered C$_2$−(C$_1$=O)−O fragments the dihedral angle of which deviates from 180°. Owing to the fixed stoichiometric relation between *sn*-1 and *sn*-2 chains, the observed effect can be only explained if the conformational disordering concerns to *sn*-1 chains as well. Water adsorption to the PC headgroups reduces the osmotic stress acting on the lipid aggregates, and as a result, the molecular packing in the membranes loosens up. We suggest that an increased fraction of CO−O−C fragments in the *sn*-1 position becomes disordered and thus, contributes to the ν_{as}^2(COC)) band as well. As a result the COG(ν_{as}(COC)) shifts downward.

Owing to the weaker hydration of the PE headgroups the RH increase affects the molecular packing in the PE bilayers to a less extend and consequently related spectral parameters as the COG(ν_{as}(COC)) but also the COG and the S_{IR} of the methylene segments remain nearly constant in the lamellar phase range at T = const. However, upon transformation into the H$_{II}$ phase, the molecular arrangement within the lipid aggregates varies distinctly. The downward shift of the COG(ν_{as}(COC)) indicates a marked disordering in the vicinity of the carbonyl ester bonds

at the *sn*-1 and *sn*-2 positions. This effect is in accordance with the negative curvature of the lipid aggregates that causes an increase of the free volume below the pivotal plane, i.e., in the region of fatty acid residues.

Interestingly, the very intense ν_{as}^1(COC)) component dominates the ν_{as}(COC) bands of the crystalline polymorphs of DTDPE (Figure 8, part a). This effect suggests a raising fraction of all-trans $C_3-C_2-C_1O-O-C$ fragments caused, for example, by a change in conformation of the glycerol backbone. Especially in the C_{II} polymorph the sharpening of the ν_{as}^1(COC)) component correlates with the sharpening of the ν(C=O) band at 1733 cm^{-1} (Figure 3) confirming the assumption of a high degree of ordering of the ester moiety probably in the *sn*-1 position. Note that this interpretation is in agreement with the assignment of the broader, less intense ν(C=O) component band at 1718 cm^{-1} to C=O groups in the *sn*-2 position which are hydrogen-bonded to amine protons of the PE headgroup.[29]

4. Summary and Conclusions

From a methodical point of view the present study demonstrates that among the solid/fluid transition also the transformation between lamellar and nonlamellar phases can be easily detected by IR spectroscopy using the linear dichroism of macroscopically oriented samples as additional criterion besides the positions of absorption bands. The type of nonlamellar phases can be identified at selected conditions using an independent method as ^{31}P NMR. FTIR is attractive because it requires only a small amount of material (<50 μg) that usually equilibrates quickly. This way the external conditions (T and RH) can be scanned quasi-continuously to detect phase transitions with high resolution.

The phase behavior of the dienic lipid DTDPE shows properties which are characteristic for PE lipids in general.[16,28] In particular, we identified the inverse hexagonal phase and a lamellar gel at higher and lower temperatures, respectively. Liquid–crystalline bilayers appear in a range of intermediate temperatures and at a high degree of hydration only. Two crystalline polymorphs can form after annealing the samples in the gel state. The chain melting transition is driven by the polymethylene parts of the tetradecadienoyl chains.

Among the phase transition ranges IR spectroscopy yields a detailed picture of the molecular arrangement, interlipid interactions and hydration of different parts of the lipid molecules. The phase states of DTDPE can be differentiated on the molecular level. The specific influence of the PE headgroup gives rise to characteristic changes of hydration and interactions between neighboring headgroups when compared with the corresponding PC, DTDPC.

The existence of the inverted hexagonal phase is somewhat unexpected because L_α/H_{II} transitions has been not detected previously for PEs lipids with effective chainlengths of $n_{eff} < 15$.[15] Moreover, the L_α/H_{II} transition appears at relatively low temperatures if compared with other PEs. These findings imply that the terminal diene groups promote the formation of nonlamellar phases. The detailed molecular interpretation of this effects should be worked out in further studies on, for example, the aggregate dimensions of DTDPE and the arrangement of the diene groups in the center of hydrophobic region.

References and Notes

(1) Chupin, V. V.; Anikin, A. V.; Serebrennikova, G. A. *Biol. Mem.* **1994**, *7*, 213.

(2) Hupfer, B.; Ringsdorf, H.; Schupp, H. *Chem. Phys. Lipids* **1983**, *33*, 355.

(3) Ohno, H.; Ogata, Y.; Tsuchida, E. *Macromolecules* **1987**, *20*, 929.

(4) Akama, K.; Morizawa, K.; Tokuyama, S.; Satoh, T.; Kobayashi, K.; Sekiguchi, S.; Tsuchida, E. *Arterial Cells, Blood Subs., Immob. Biotechnol.* **1994**, *22*, 901.

(5) Okahata, Y.; Ariga, K.; Seki, T. *J. Am. Chem. Soc.* **1988**, *110*, 2495.

(6) Regen, S. L.; Shin, J.-S. *J. Am. Chem. Soc.* **1984**, *106*, 5756.

(7) Seki, N.; Tsuchida, E.; Ukaji, K.; Sekiya, T.; Nozawa, Y. *Polym. Bull.* **1985**, *13*, 489.

(8) Ohno, H.; Takeoka, S.; Tsuchida, E. E. *Polym. Bull. (Berlin)* **1985**, *14*, 487.

(9) Blume, A. *Chem. Phys. Lipids* **1991**, *57*, 253.

(10) Lee, Y.-S.; Yang, J.-Z.; Sisson, T. M.; Frankel, D. A.; Gleeson, J. T.; Aksay, E.; Keller, S. L.; Gruner, S. M.; O'Brien, D. F. *J. Am. Chem. Soc.* **1995**, *117*, 5573.

(11) Srisiri, W.; Sisson, T. M.; O'Brien, D. F. O.; McGrath, K. M.; Han, Y.; Gruner, S. M. *J. Am. Chem. Soc.* **1997**, *119*, 4866.

(12) Binder, H.; Anikin, A.; Kohlstrunk, B.; Klose, G. *J. Phys. Chem. B* **1997**, *101*, 6618.

(13) Binder, H.; Gutberlet, T.; Anikin, A.; Klose, G. *Biophys J.* **1998**, *74*, 1908.

(14) Anikin, A.; Chupin, V.; Anikin, M.; Serebrennikova, G.; Tarahovsky, J. *Makromol. Chem.* **1993**, *194*, 2663.

(15) Lewis, R. N. A. H.; Mannock, D. A.; McElhaney, R. N.; Turner, D. C.; Gruner, S. M. *Biochemistry* **1989**, *28*, 541.

(16) Seddon, J. M.; Cevs, G.; Marsh, D. *Biochemistry* **1983**, *22*, 1280.

(17) Mädler, B.; Binder, H.; Klose, G. *J. Colloid Interface Sci.* **1998**, *124–138*.

(18) Binder, H.; Anikin, A.; Kohlstrunk, B. *J. Phys. Chem. B* **1999**, *103*, xxxx.

(19) Fringeli, U. P.; Günthard, H. H. *Mol. Biol., Biochem. Biophys.* **1981**, *31*, 270.

(20) Schröder, H.; Neuroth, N. *Optik* **1967**, *26*, 381.

(21) Flach, C. R.; Gericke, A.; Mendelsohn, R. *J. Phys. Chem. B* **1997**, *101*, 58.

(22) Harrick, N. J.; Internal Reflection Spectroscopy, Wiley: New York, 1967.

(23) Hübner, W.; Mantsch, H. H. *Biophys J.* **1991**, *59*, 1261.

(24) Schäfer, H.; Mädler, B.; Volke, F. *J. Magn. Reson.* **1995**, *A116*, 145.

(25) Snyder, R.; Strauss, G. H.; Elliger, C.; A. *J. Phys. Chem.* **1982**, *86*, 5145.

(26) Casal, H. L.; Mantsch, H. H. *Biochim. Biophys. Acta* **1984**, *779*, 381.

(27) Cevc, G.; Marsh, D. *Phospholipid Bilayers. Physical Principles and Models*; John Wiley and Sons: New York, 1987.

(28) Seddon, J. M. *Biochim. Biophys. Acta* **1990**, *1031*, 1.

(29) Lewis, R. N. A. H.; McElhaney, R. N. *Biophys J.* **1993**, *64*, 1081.

(30) Harlos, K.; Eibel, H. *Biochemistry* **1981**, *20*, 2888.

(31) Mantsch, H. H.; Martin, A.; Cameron, D. G. *Biochemistry* **1981**, *20*, 3138.

(32) Mantsch, H. H.; Hsi, S. C.; Butler, K. W.; Cameron, D. G. *Biochim. Biophys. Acta* **1983**, *728*, 325.

(33) Hauser, H.; Pascher, I.; Pearson, R. H.; Sundell, S. *Biochim. Biophys. Acta* **1981**, *650*, 21.

(34) Hitchcock, P. B.; Mason, R.; Thomas, K. M.; Shipley, G. G. *Proc. Natl. Acad. Sci. U.S.A.* **1974**, *71*, 3036.

(35) Blume, A.; Hübner, W.; Messner, G. *Biochemistry* **1988**, *27*, 8239.

(36) Lewis, R. N. A. H.; McElhaney, R. N. *Biophys J.* **1992**, *61*, 63.

(37) Cevc, G.; In, *Lipid Hydration*; Westhof, E., Ed.; Boca Raton, FL, 1993.

(38) Pohle, W.; Selle, C. *Chem. Phys. Lipids* **1996**, *82*, 191.

(39) Campbell, R. F.; Meirovich, E.; Freed, J. *J. Phys. Chem.* **1979**, *83*, 525.

(40) Seelig, J. *Biochim. Biophys. Acta* **1978**, *515*, 105.

(41) Gruner, S. M.; Cullis, P. R.; Hope, M. J.; Tilcock, C. P. S. *Annu. Rev. Biophys. Biophys. Chem.* **1985**, *14*, 311.

(42) Cullis, P. R.; de Kruijff, B. *Biochim. Biophys. Acta* **1976**, *436*, 523.

(43) Gawrisch, K.; Parsegian, V. A.; Hajduk, D. A.; Tate, M. W.; Gruner, S. M.; Fuller, N. L.; Rand, R. P. *Biochemistry* **1992**, *31*, 2856.

(44) Hsieh, C.-H.; Sue, S.-C.; Lyu, P.-C.; Wu, W.-G. *Biophys. J.* **1997**, *73*, 870.

(45) Seddon, J. M.; Cevc, G.; Kaye, R. D.; Marsh, D. *Biochemistry* **1984**, *23*, 2634.

(46) Gleeson, J. T.; Erramilli, S.; Gruner, S. M. *Biophys J.* **1994**, *67*, 706.

(47) Ulrich, A.; Sami, M.; Watts, A. *Biochim. Biophys. Acta* **1994**, *1191*, 225.

Phospholipids with Terminal Diene Groups

J. Phys. Chem. B, Vol. 103, No. 3, 1999 **471**

(48) Kozlov, M. M.; Leikin, S.; Rand, R. P. *Biophys J.* **1994**, *67*.

(49) Marsh, D.; Seddon, J. M. *Biochim. Biophys. Acta* **1982**, *690*, 117.

(50) Fringeli, U. P.; Günthard, H. H. *Biochim. Biophys. Acta* **1976**, *450*, 101.

(51) Nilsson, A.; Holmgren, A.; Lindblom, G. *Biochemistry* **1991**, *30*, 2126.

(52) Grdadolnik, J.; Kidric, J.; Hadzi, D. *Chem. Phys. Lipids* **1991**, *59*, 57.

(53) Blume, A.; Hübner, W.; Müller, M.; Bauerle, H. *Ber. Bunsen-Ges. Phys. Chem.* **1988**, *92*, 964.

(54) Lewis, R. N. A. H.; McElhaney, R. N.; Pohle, W.; Mantsch, H. *Biophys. J.* **1994**, *67*, 2367.

(55) Arrondo, J. L. R.; Goni, F. M.; Macarulla, J. M. *Biochim. Biophys. Acta* **1984**, *794*, 165.

(56) Castresana, J.; Nieva, J.-L.; Rivas, E.; Alonso, A. *Biochem. J.* **1992**, *282*, 467.

(57) Cheng, K. H. *Chem. Phys. Lipids* **1991**, *60*, 119.

(58) Nilsson, A.; Holmgren, A.; Lindblom, G. *Chem. Phys. Lipids* **1994**, *71*, 119.

(59) Bradbury, E. M.; Eliott, A.; Fraser, R. D. B. *Trans. Faraday Soc.* **1960**, *56*, 1117.

(60) Fringeli, U. P.; Müldner, H. G.; Günthard, H. H.; Gasche, W.; Leuzinger, W. *Z. Naturforsch.* **1972**, *27b*, 780.

(61) Pascher, I.; Lundmark, M.; Nyholm, P.-G.; Sundell, S. *Biochim. Biophys. Acta* **1992**, *1113*, 339.

(62) Hübner, W.; Mantsch, H. H.; Casal, H. L. *Appl. Spectrosc.* **1990**, *44*, 732.